Stability of gravity-driven free-surface flow past a deformable solid: The role of depth-dependent modulus

Shraddha Mandloi and V. Shankar*
Department of Chemical Engineering, Indian Institute of Technology, Kanpur 208016, India

(Received 25 December 2019; accepted 28 March 2020; published 23 April 2020)

The linear stability of a Newtonian liquid layer flowing down an inclined plane lined with a deformable linear elastic solid characterized by a continuously varying modulus is analyzed in this study. A low-wave-number asymptotic analysis is performed to obtain an analytical expression for the complex wavespeed which shows striking similarity with the earlier results of Sahu and Shankar [Sahu and Shankar, Phys. Rev. E **94**, 013111 (2016)] for gravity-driven flow of Newtonian fluid past a solid bilayer having constant shear modulus (in each layer) lined on a rigid inclined plane. This shows that a deformable solid layer having a continuously varying shear modulus can be treated as a generalization of a system having multiple solid layers of constant shear modulus. Also, in the low-wave-number limit, we show that the stability of the free surface is governed by the value of effective shear modulus G_{eff}, and not by the detailed spatial variation of the modulus. Here the effective shear modulus ($H/G_{\text{eff}} = \int_1^{1+H} 1/[E_0 + \overline{E}(z)]dz$, where $[E_0 + \overline{E}(z)]$ represents the modulus gradient function) characterizes the overall modulus of the elastic solid, which is obtained by treating the continuous variation to be the limit of the arrangement of solid layers of infinitesimal thickness (each having a constant shear modulus) in a series. At finite wave numbers, we show that the free-surface and the liquid-solid interface become unstable as we increase the value of Γ, where Γ indicates the ratio of viscous stresses in the fluid to elastic stresses in the solid. When the system is analysed for different types of spatial modulus variations, we find results similar to those of Gkanis and Kumar [Gkanis and Kumar, Phys. Rev. E **73**, 026307 (2006)], i.e., when we have two different configurations of the shear modulus function that have the same spatially averaged modulus, but have different values at the interface, the system is more stable for the configuration having higher shear modulus at the liquid-solid interface. In a similar manner, when we examined systems having the same shear modulus at the liquid-solid interface and same average modulus, the more stable case is the one which has a higher value of shear modulus just below the interface. Thus the use of deformable solids with a depth-dependent modulus potentially offers more control in the passive manipulation of the instabilities.

DOI: 10.1103/PhysRevE.101.043107

I. INTRODUCTION

Gravity-driven free surface flow of liquid layers past a rigid inclined plane has been a topic of interest since the pioneering work of Benjamin [1] and Yih [2]. Yih showed that flow down a rigid inclined plane becomes unstable in low-wave-number regime as the Reynolds number increases beyond a critical value for a given angle of inclination. Later, the role of viscosity stratification [3] was examined for two-layer flow of fluid down a rigid inclined plane [4–7], which showed that the interaction between the two interfaces makes the flow unstable even at zero Reynolds number. Recently, there has been renewed interest in the understanding of the stability of flow of a liquid layer past a deformable solid layer [8,9], as it is relevant to many practical applications, viz., coating processes, flow in microfluidic devices, and so on. In addition, it aids in the understanding of a large variety of biologically significant phenomena such as the flow of blood in blood vessels [10] and circulation of air in the pulmonary system [11]. The interaction of multiple layers gives rise to interfacial instabilities, which may or may not be desirable for the application under consideration. Hence, it is important to manipulate (either induce or suppress) the interfacial instabilities. Prior studies [12–14] analyzed "active manipulation" strategies such as imposing wall oscillations and the heating of the inclined plane. However, it is possible to conveniently control these instabilities using the deformability of solid layers [15–20]. This "passive manipulation" technique controls the interfacial instabilities without any external interventions, such as forced oscillations. Though many earlier studies of interest assumed the shear modulus of the solid to be a constant [15–17,20–22], however, variation in the shear modulus with depth is observed to be present in many practical cases. For example, vertical gradients in the modulus are formed during the curing of a polymer gel and a high-modulus protective coating is used to prevent damage to the solid [23]. Functionally graded materials are generally used in severe operating conditions (high temperature, high pressure, high abrasive conditions) to prevent damage to solids. Further, biological conduits (such as blood vessels) are made of multiple layers of varying moduli [24] and can be modeled using a depth-dependent modulus. Hence, the purpose of this work is to investigate the role of depth-dependent shear modulus on the stability of fluid flow past a deformable solid lined on a rigid inclined plane.

*Corresponding author: vshankar@iitk.ac.in

Kumaran *et al.* [8] analyzed the stability of a plane Couette flow past a linear viscoelastic solid [25] in the creeping-flow limit and found that if the dimensionless strain in the solid exceeds a critical value, the flow becomes unstable. This instability is referred to as the "liquid-solid" (LS) interfacial mode henceforth in this study. Evidently, this interfacial mode is expected to be present even if there are two or more layers of liquid adjacent to the solid. For free-surface flow past a deformable linear elastic solid having a constant shear modulus, Shankar and Sahu [16] showed that the deformability of the solid layer can be used to suppress free surface instability, henceforth referred to as the "gas-liquid" (GL) interfacial mode, in the long-wave limit. However, at finite wave numbers, an increase in the value of the nondimensional parameter Γ (which represents the ratio of viscous stress in the fluid to the elastic stress in the solid) above a critical value destabilizes the flow, but there is a sufficient window where both the GL and LS modes remained stable at all wave numbers. Thus, in practice, it is possible to tune the parameters such as shear modulus and thickness of the solid so that the free-surface instability is fully suppressed. The configuration used by Shankar and Sahu [16] was further analyzed using the neo-Hookean solid model by Gkanis and Kumar [15], in the creeping-flow limit. They showed that the presence of a free surface has a stabilizing effect on the stability of flow past a deformable elastic solid. This work was further extended to finite Reynolds numbers by Gaurav and Shankar [17]. They showed that the deformability of the solid layer aids in suppressing the free-surface instability for both solid models (linear viscoelastic and neo-Hookean) at all wavelengths. Thus, there exists a significant window in the shear modulus of the solid considered, for moderate values of solid thickness, where both modes remain stable for all wave numbers. Gkanis and Kumar [26] carried out a linear stability analysis to examine the role of a depth-dependent modulus on the stability of the Couette flow of a Newtonian fluid past a linear elastic solid, in the zero Reynolds number limit. They considered the modulus of the solid to be a continuous function of position and showed that, if the average modulus (defined as the spatial average of the modulus function) is the same, then the system with the higher modulus close to the interface is more stable as compared to the one with higher modulus close to the rigid bottom surface. The subsequent experimental work of Neelamegam *et al.* [27] on plane Couette flow considered a solid bilayer, and it showed that the solid layer adjacent to the liquid layer has a dominant effect on the liquid-solid interfacial instability, in broad agreement with the predictions of Gkanis and Kumar [15].

In a recent study, Sahu and Shankar [20] analyzed the effect of the flow of Newtonian fluid down an inclined plane lined with a linear viscoelastic solid bilayer. A long-wave asymptotic analysis demonstrated that the stability of the free-surface mode is insensitive to the nature of the solid adjacent to the liquid layer. Instead, it was shown that it is the effective shear modulus of the bilayer G_{eff} (defined as $H/G_{\text{eff}} = H_1/G_1 + H_2/G_2$, where H_1 and H_2 represent the thickness of the solid layers, and G_1 and G_2 are the shear moduli of the deformable solid layers) that determines the stability of the free surface in the long-wave limit. However, at finite wave numbers, the results indicate that additional instabilities at the free surface and the liquid-solid interface can be induced by wall deformability and inertia in the fluid and solid. Interestingly, the onset of these additional instabilities is sensitive to the relative placements of the two solid layers comprising the bilayer.

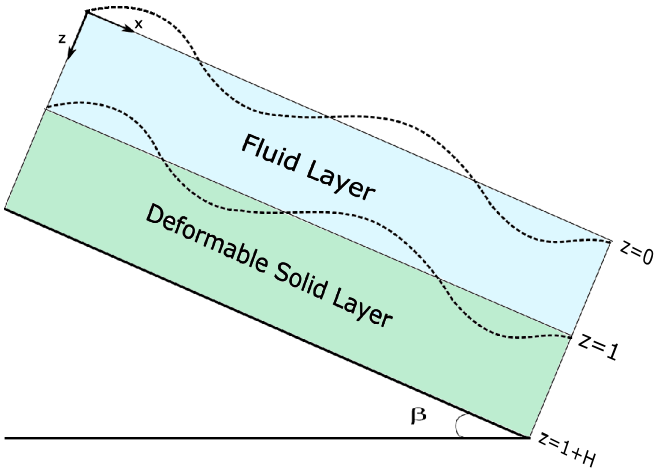

FIG. 1. Schematic diagram showing the system under consideration with nondimensional coordinates.

In the present work, we explore the possibility of using a linear elastic solid with depth-dependent elasticity modulus as a possible candidate for manipulating the free-surface instability. In what follows, we carry out a linear stability analysis for a liquid layer flowing down an inclined plane, where the rigid surface of the inclined plane is lined with the deformable solid layer with depth-dependent shear modulus. In this study we restrict ourselves to the simpler linear elastic model as compared to the more complete neo-Hookean model of a solid so as to demonstrate the qualitative behavior of free-surface and liquid-solid interfacial instability with respect to the deformation in the solid layer with variable modulus. Also, as shown by the earlier study of Gaurav and Shankar [17], for a single-layer elastic solid, the results from the neo-Hookean model are in qualitative agreement with those predicted using the linear elastic model [16]. We also thereby extend the earlier study of Sahu and Shankar [20] to the case of a solid layer with depth-dependent shear modulus.

The rest of this paper is divided into four sections. Section II describes the governing equations and the associated boundary conditions, along with the base-state solutions. Section III describes the low-wave-number asymptotic analysis which determines the stability criterion of the GL mode in the long-wave limit. Section IV presents the results obtained by numerically solving the set of governing equations at arbitrary wave numbers. Finally, we end with the main conclusions of this study in Sec. V.

II. PROBLEM FORMULATION

A. Governing equations

We consider the flow of an incompressible Newtonian liquid layer past an impermeable linear elastic solid with a continuously varying shear modulus as shown in Fig. 1. The deformable solid is assumed to be perfectly bonded to the

rigid surface at $z^* = (1 + H)R$, which is inclined at an angle β with the horizontal. The liquid layer (viscosity μ) flows over the deformable solid layer in the region $0 < z^* < R$ under the influence of gravity and is exposed to a passive gas at the free surface $z^* = 0$. Here the superscript * has been used for denoting dimensional variables. The density of the solid layer is assumed to be comparable to that of the liquid layer (ρ) and hence the ratio of the densities is assumed to be unity in this work. For small density differences, qualitative predictions of the present study will remain the same [16].

In the base state, we consider a unidirectional, steady, and fully developed flow in the x direction. The deformable solid layer is considered to be at rest and the interfaces are assumed to be flat. The base-state velocity profile in the liquid layer is given as

$$\bar{v}_x(z^*) = \frac{\rho g \sin\beta}{2\mu}(R^2 - z^{*2}). \tag{1}$$

The average velocity of the flow in the liquid layer is $\overline{V_a} = \rho g R^2 \sin\beta/3\mu$. Various dynamical variables are nondimensionalized using the following scales: thickness of the fluid R is used for lengths and displacements, the average velocity of the laminar flow $\overline{V_a}$ is used for velocities, $R/\overline{V_a}$ for time, and $\mu\overline{V_a}/R$ for stresses and pressure. The nondimensional velocity and pressure fields in the liquid layer under laminar conditions are given by

$$\bar{v}_x = \tfrac{3}{2}(1 - z^2), \tag{2}$$

$$\bar{p} = 3\,z\cot\beta. \tag{3}$$

The base-flow quantities are henceforth denoted by an overbar. Fluid flow is governed by the following dimensionless Navier-Stokes mass and momentum balance equations:

$$\partial_x v_x + \partial_z v_z = 0, \tag{4}$$

$$\mathrm{Re}[\partial_t + v_x\partial_x + v_z\partial_z]v_x = -\partial_x p + 3 + \nabla^2 v_x, \tag{5}$$

$$\mathrm{Re}[\partial_t + v_x\partial_x + v_z\partial_z]v_z = -\partial_z p + 3\cot\beta + \nabla^2 v_z, \tag{6}$$

where $\partial_t = \partial/\partial t$ and similar definitions are valid for ∂_x, ∂_z, and $\nabla^2 = (\partial_x^2 + \partial_z^2)$. For the present study, we neglect variation of any dynamic quantity in the y direction and limit ourselves to two-dimensional disturbances in the x-z plane. The Reynolds number in Eqs. (5) and (6) is defined as $\mathrm{Re} = \rho\bar{V}_a R/\mu$. The total stress tensor in the liquid layer can be written as $T_{ij} = -p\,\delta_{ij} + \tau_{ij}$, where p is the isotropic pressure and $\tau_{ij} = (\partial_i v_j + \partial_j v_i)$ is the deviatoric stress tensor for the Newtonian liquid.

The solid is considered to be linear elastic and the dynamical fluctuations in the solid layer are governed by displacement field $\mathbf{u}$, which represents the deviation of material points from their base-state positions. The velocity field in the solid layer is given by $\mathbf{v} = \partial_\mathbf{t}\mathbf{u}$. The total stress tensor in the solid layer Π_{ij}, is given as $\Pi_{ij} = -p_s\,\delta_{ij} + \sigma_{ij}$, where p_s is the isotropic pressure, and $\sigma_{ij} = [E_0 + \overline{E}(z)](\partial_i u_j + \partial_j u_i)$ is the deviatoric stress tensor and $[E_0 + \overline{E}(z)]$ represents the modulus gradient function.

The incompressible solid layer satisfies the following nondimensionalized governing equations

$$0 = \partial_x u_x + \partial_z u_z, \tag{7}$$

$$\mathrm{Re}\partial_t^2 u_x = -\partial_x p_s + 3 + \frac{2}{\Gamma}\partial_x\{[1 + E(z)]\partial_x u_x\} + \frac{1}{\Gamma}\partial_z\{[1 + E(z)](\partial_z u_x + \partial_x u_z)\}, \tag{8}$$

$$\mathrm{Re}\partial_t^2 u_z = -\partial_z p_s + 3\cot\beta + \frac{2}{\Gamma}\partial_z\{[1 + E(z)]\partial_z u_z\} + \frac{1}{\Gamma}\partial_x\{[1 + E(z)](\partial_z u_x + \partial_x u_z)\}. \tag{9}$$

Here the nondimensional parameter $\Gamma = \frac{\overline{V_a}\mu}{E_0 R}$, represents the ratio of viscous force in the fluid to elastic force in the solid and $E(z) = \frac{\overline{E}(z)}{E_0}$ is the nondimensional shear modulus. For a fixed set of R, $\overline{V_a}$ and μ, $\Gamma \to 0$ in the limit of rigid solid layer ($E_0 \sim 10^{11}$ Pa).

To solve the above set of equations, we use no-slip boundary conditions at $z = (1 + H)$ as the solid layer is assumed to be perfectly bonded to a rigid, impermeable inclined plane. At the perturbed liquid-solid interface ($z = 1$) and gas-liquid interface ($z = 0$), the continuity of normal and tangential velocities and stresses are applied. In additions, the position of the gas-liquid interface follows the kinematic condition

$$\partial_t h + v_x\partial_x h = v_z. \tag{10}$$

B. Linear stability analysis

The stability of the coupled fluid-solid system is examined by using a linear stability analysis where small perturbations (denoted by primed quantities) are imposed on a given physical quantity as $\phi = \bar{\phi} + \phi'$ and the variables in the fluid and the solid layer are similarly perturbed. A temporal linear stability analysis is performed to determine the evolution of these small perturbations. The perturbed quantities are represented in the form of Fourier modes in the x direction, with an exponential dependence in time

$$\phi'(x, z, t) = \tilde{\phi}(z)\exp[ik(x - ct)], \tag{11}$$

where ϕ' represents perturbed dynamical variables in the fluid and solid layers, k is the wave number which is inversely proportional to the wavelength of perturbations, c is the complex wavespeed that determines the growth of perturbations, and $\tilde{\phi}(z)$ represents the eigenfunctions which are to be determined from the linearized differential equations governing the stability of the system. Any variations in the y direction are neglected and hence, only two-dimensional perturbations are imposed to analyze the stability of the system. The complex wavespeed $c = c_r + ic_i$, where c_r denotes the phase velocity of perturbations, and c_i dictates the growth or decay of perturbations. If $c_i > 0$, the perturbations will grow with time and the given base state will be temporally unstable.

The linearized equations for the fluid around the base state [Eq. (2)] can be obtained by substituting the Fourier mode representation [Eq. (11)] in the governing Eqs. (4) to (9).

The linearized governing equations for the liquid layer are as follows:

$$d_z\tilde{v}_z + ik\tilde{v}_x = 0, \tag{12}$$

$$\mathrm{Re}[ik(\bar{v}_x - c)\tilde{v}_x + (d_z\bar{v}_x)\tilde{v}_z] = -ik\tilde{p} + \left(d_z^2 - k^2\right)\tilde{v}_x, \tag{13}$$

$$\mathrm{Re}[ik(\bar{v}_x - c)\tilde{v}_z] = -d_z\tilde{p} + \left(d_z^2 - k^2\right)\tilde{v}_z. \tag{14}$$

The above equations are combined to give a fourth-order ordinary differential equation, which is essentially the Orr-Sommerfeld equation for the dynamical variable $\tilde{v}_z$:

$$ik\mathrm{Re}\left[(\bar{v}_x - c)\left(d_z^2 - k^2\right) - d_z^2\bar{v}_x\right]\tilde{v}_z = \left(d_z^2 - k^2\right)^2\tilde{v}_z. \tag{15}$$

The linearized stability equations for the displacement field in the upper solid layer are as follows:

$$0 = d_z\tilde{u}_z + ik\tilde{u}_x, \tag{16}$$

$$-\mathrm{Re}k^2c^2\tilde{u}_x = -ik\tilde{p}_s + \frac{1}{\Gamma}\frac{dE(z)}{dz}(ik\tilde{u}_z + d_z\tilde{u}_x) + \frac{1}{\Gamma}[1 + E(z)]\left(d_z^2 - k^2\right)\tilde{u}_x, \tag{17}$$

$$-\mathrm{Re}k^2c^2\tilde{u}_z = -d_z\tilde{p}_s + \frac{1}{\Gamma}\left\{[1 + E(z)]\left(d_z^2 - k^2\right)\tilde{u}_z\right\} + \frac{2}{\Gamma}\frac{dE(z)}{dz}(d_z\tilde{u}_z). \tag{18}$$

These equations can further be combined to obtain a fourth-order differential equation, which is as follows:

$$[1 + E(z)]\left(d_z^2 - k^2\right)^2\tilde{u}_z + 2\frac{dE(z)}{dz}\left(d_z^3 - d_zk^2\right)\tilde{u}_z + \frac{d^2E(z)}{dz^2}\left(d_z^2 + k^2\right)\tilde{u}_z + \mathrm{Re}k^2c^2\Gamma\left(d_z^2 - k^2\right)\tilde{u}_z = 0. \tag{19}$$

Now, by substituting $h(x,t) = \tilde{h}\exp[ik(x - ct)]$ and by linearizing the other quantities about $z = 0$, we can express the kinematic equation (10) in terms of Fourier modes as

$$ik(\bar{v}_x|_{z=0} - c)\tilde{h} = \tilde{v}_z|_{z=0}, \tag{20}$$

Here $\tilde{h}$ represents the evolution of the position of gas-liquid interface. The linearized boundary conditions at $z = 0$, i.e., the normal stress and the tangential stress conditions are obtained by Taylor-expanding the boundary conditions about $z = 0$, to give

$$-3\tilde{h} + (d_z\tilde{v}_x + ik\tilde{v}_z) = 0, \tag{21}$$

$$-\tilde{p} - 3\tilde{h}\cot\beta + 2d_z\tilde{v}_z = 0. \tag{22}$$

The velocity and stress continuity conditions are linearized about the interface $z = 1$ which gives

$$\tilde{v}_z = -ikc\tilde{u}_z, \tag{23}$$

$$\tilde{v}_x + d_z\bar{v}_x|_{z=1}\tilde{u}_z = -ikc\tilde{u}_x, \tag{24}$$

$$d_z\tilde{v}_x + ik\tilde{v}_z = \frac{1}{\Gamma}[1 + E(1)][d_z\tilde{u}_x + ik\tilde{u}_z], \tag{25}$$

$$-\tilde{p} + 2d_z\tilde{v}_z = -\tilde{p}_s + \frac{2}{\Gamma}[1 + E(1)]d_z\tilde{u}_z. \tag{26}$$

Here the position of the interface is represented as $\tilde{g} = \tilde{u}_z|_{z=1}$, consistent with the assumptions of linear stability analysis. The boundary conditions for the lower solid layer at $z = 1 + H$ are simply zero-displacement conditions

$$\tilde{u}_z = 0, \quad \tilde{u}_x = 0. \tag{27}$$

This completes the specification of the stability problem for the two-layer configuration of interest. The complex wavespeed c is an unknown eigenvalue which is a function of Re, k, Γ, β, H, and μ. The linearized equations are solved numerically, for arbitrary values of k and Re. A long-wave asymptotic analysis is performed for the present problem, along the lines of Shankar and Sahu [16], to understand the effect of the depth-dependent shear modulus of the deformable solid on the stability of the system in low-k limit. Also, this analysis will provide us with the analytical solution in the long-wave limit, which can further be extended to finite k region using the numerical solution.

III. LOW-WAVE-NUMBER ASYMPTOTIC ANALYSIS

In this section we present the results obtained by performing a low-wave-number asymptotic analysis [16]. Specifically, we focus on the effect of the continuously varying modulus of the deformable solid on the free-surface instability. This analysis is valid if the wavelength of the disturbances is large as compared to all cross-stream widths, and k satisfies the condition, i.e., $k \ll 1/(1 + H)$. When H is an $O(1)$ quantity, this relation reduces to $k \ll 1$, on the other hand, for $H \gg 1$, this relation is satisfied if $k \ll 1/H$. Thus, for larger values of H, the analysis is valid for much smaller k values. In our analysis, we restrict H to $O(1)$, so the limit $k \ll 1$ is considered here. In this limit, the complex wavespeed is expanded in an asymptotic series in k as

$$c = c^{(0)} + k\,c^{(1)} + \cdots. \tag{28}$$

In this study, the leading order and the $O(k)$ correction to the wavespeed are sufficient to determine the stability of the disturbances in low-wave-number regime as shown later in this section. Further, we assumed $\tilde{v}_z$ to be an $O(1)$ quantity, which leads to $\tilde{v}_x \sim O(k^{-1})$ from the continuity equation (12) and $\tilde{p} \sim O(k^{-2})$ from the x-momentum equation (13). The expansions of the above terms are as follows:

$$\tilde{v}_z = \tilde{v}_z^{(0)} + k\tilde{v}_z^{(1)} + \cdots, \tag{29}$$

$$\tilde{v}_x = k^{-1}\tilde{v}_x^{(0)} + \tilde{v}_x^{(1)} + \cdots, \tag{30}$$

$$\tilde{p} = k^{-2}\tilde{p}^{(0)} + k^{-1}\tilde{p}^{(1)} + \cdots. \tag{31}$$

Similarly, displacement and pressure field for the solid layer are expanded as

$$\tilde{u}_z = \tilde{u}_z^{(0)} + k\tilde{u}_z^{(1)} + \cdots, \tag{32}$$

$$\tilde{u}_x = k^{-1}\tilde{u}_x^{(0)} + \tilde{u}_x^{(1)} + \cdots, \tag{33}$$

$$\tilde{p}_s = k^{-2}\tilde{p}_s^{(0)} + k^{-1}\tilde{p}_s^{(1)} + \cdots. \tag{34}$$

The free-surface height fluctuation is expanded as

$$\tilde{h} = k^{-1}\tilde{h}^{(0)} + \tilde{h}^{(1)} + \cdots. \tag{35}$$

Now, to understand the leading order dynamics of the system, we substitute the above expansions of the perturbed dynamical quantities in the governing equations for fluid and solid layer (15) to (18) and get

$$d_z^4 \tilde{v}_z^{(0)} = 0, \tag{36}$$

$$\frac{d}{dz}\left[\left(\frac{1+E(z)}{\Gamma}\right)\frac{d\tilde{u}_x^{(0)}}{dz}\right] = 0. \tag{37}$$

The general solution to the fourth-order differential equation governing the leading order dynamics of the fluid velocity field (36) is given as

$$\tilde{v}_z^{(0)} = A_1 + A_2 z + A_3 z^2 + A_4 z^3. \tag{38}$$

As the leading-order ordinary differential equation for fluid (36) is linear and homogeneous, we determine the eigenfunction $\tilde{v}_z^{(0)}$ only up to a multiplicative constant. Therefore, we set $A_1 = 1$ without any loss of generality. The constants A_2, A_3, and A_4 can be determined by substituting the asymptotic expansions [Eqs. (28) to (35)] in the boundary conditions [Eqs. (20) to (27)]. The leading-order boundary conditions at the gas-liquid interface, $z = 0$, obtained are

$$i\big[\bar{v}_x|_{z=0} - c^{(0)}\big]\tilde{h}^{(0)} = \tilde{v}_z^{(0)}, \tag{39}$$

$$-3\tilde{h}^{(0)} + d_z \tilde{v}_x^{(0)} = 0, \tag{40}$$

$$-\tilde{p}^{(0)} = 0. \tag{41}$$

Similarly, the leading-order boundary conditions at the fluid-solid interface, $z = 1$, are:

$$\tilde{v}_z^{(0)} = 0, \tag{42}$$

$$\tilde{v}_x^{(0)} = 0, \tag{43}$$

$$d_z \tilde{v}_x^{(0)} = \frac{1+E(z)}{\Gamma}\, d_z \tilde{u}_x^{(0)}, \tag{44}$$

$$\tilde{p}^{(0)} = \tilde{p}_s^{(0)}\,. \tag{45}$$

Interestingly, the no-slip boundary conditions at the liquid-solid interface [Eqs. (42) and (43)] suggest that the solid deformability does not have any impact on the fluid velocity field $(\tilde{v}_x^{(0)}, \tilde{v}_z^{(0)})$ to the leading order as it is identical to the velocity field for flow past rigid inclined planes. However, the fluid velocity field at the leading order shears the deformable solid layer via the tangential stress balance condition at the fluid-solid interface [Eq. (44)], that leads to the deformation in the solid layer at the leading order. Lastly, the leading-order boundary conditions at $z = (1 + H)$ are

$$\tilde{u}_z^{(0)} = 0, \quad \tilde{u}_x^{(0)} = 0. \tag{46}$$

The solutions to the leading-order dynamical variables of the liquid layer are

$$\tilde{v}_z^{(0)} = (z-1)^2\,, \tag{47}$$

$$\tilde{v}_x^{(0)} = 2i(z-1)\,, \tag{48}$$

$$\tilde{p}^{(0)} = 0\,. \tag{49}$$

The free-surface height fluctuation at $z = 0$, to a leading order, could be found using Eq (41):

$$\tilde{h}^{(0)} = 2i/3. \tag{50}$$

Therefore, the leading-order wavespeed is obtained using the linearized kinematic condition (39), given as

$$c^{(0)} = 3. \tag{51}$$

This matches with Yih's [2] result for the flow of a liquid film down an rigid inclined plane. Since the flow is neutrally stable to the leading order, the stability of the system would be determined from the first correction to the wavespeed. For subsequent analysis, we require the leading-order deformation field in the solid layer, which can be determined by using Eq. (37) and the boundary conditions (44) and (46):

$$\tilde{u}_x^{(0)} = -2i\Gamma \int_z^{1+H} \frac{dz'}{1+E(z')}, \tag{52}$$

$$\tilde{u}_z^{(0)} = -2\Gamma \int_1^z \int_z^{1+H} \left[\frac{dz'}{1+E(z')}\right] dz''. \tag{53}$$

$$\tilde{p}_s^{(0)} = 0. \tag{54}$$

With these solutions, we now proceed to calculate the first correction to the wavespeed $c^{(1)}$.

The $O(k)$ equation for the velocity field $\tilde{v}_z$, obtained by substituting the asymptotic expansions in the Orr-Sommerfeld equation (15) for the dynamical variable $\tilde{v}_z$, is

$$d_z^4 \tilde{v}_z^{(1)} = i\mathrm{Re}\big[(\bar{v}_x - c^{(0)})d_z^2 \tilde{v}_z^{(0)} - (d_z^2 \bar{v}_x)\tilde{v}_z^{(0)}\big]. \tag{55}$$

The general solution to this inhomogeneous fourth-order differential Eq. (55) is given as

$$\tilde{v}_z^{(1)} = B_1 + B_2 z + B_3 z^2 + B_4 z^3 - \frac{i\mathrm{Re}}{20} z^5. \tag{56}$$

Here the constant $B_1 = 0$, as we have fixed the amplitude of $\tilde{v}_z$ at $z = 0$ to be 1 by setting the coefficient A_1 at leading order to be 1. The constants, B_2, B_3, and B_4, are determined by first correction to the boundary conditions at $z = 0$ and $z = 1$ [Eqs. (20) to (23)]. At the free surface, i.e., $z = 0$, the first correction to the linearized kinematic equation is given as

$$i\big[\bar{v}_x|_{z=0} - c^{(0)}\big]\tilde{h}^{(1)} - ic^{(1)}\tilde{h}^{(0)} = \tilde{v}_z^{(1)}\big|_{z=0}. \tag{57}$$

The first correction to the continuity of tangential and normal stresses at $z = 0$ is given as

$$-3\tilde{h}^{(1)} + d_z \tilde{v}_x^{(1)} = 0, \tag{58}$$

$$-\tilde{p}^{(1)} - 3\tilde{h}^{(0)} \cot\beta = 0. \tag{59}$$

At the solid-liquid interface $z = 1$, the velocity continuity conditions at order $O(k)$ are

$$\tilde{v}_z^{(1)} = -ic^{(0)}\tilde{u}_z^{(0)}, \tag{60}$$

$$\tilde{v}_x^{(1)} + d_z \bar{v}_x|_{z=1}\tilde{u}_z^{(0)} = -ic^{(0)}\tilde{u}_x^{(0)}. \tag{61}$$

These equations (59) to (61) are used to determine the $O(k)$ component of the perturbed velocity field. The solution for

$\tilde{v}_z^{(1)}$ is as follows:

$$\tilde{v}_z^{(1)} = i\left[\frac{7}{2}\mathrm{Re} - \frac{\cot\beta}{3} - 6\Gamma\int_1^{1+H}\frac{dz'}{1+E(z')}\right]z + i\left[\frac{-4}{5}\mathrm{Re} + \frac{2}{3}\cot\beta + 6\Gamma\int_1^{1+H}\frac{dz'}{1+E(z')}\right]z^2 + i\left[\frac{\mathrm{Re}}{2} - \frac{\cot\beta}{3}\right]z^3 - i\frac{\mathrm{Re}}{20}z^5. \quad (62)$$

The first correction to the height fluctuation $\tilde{h}^{(1)}$ obtained from Eq. (58) is

$$\tilde{h}^{(1)} = \frac{8}{15}\mathrm{Re} - \frac{4}{9}\cot\beta - 4\Gamma\int_1^{1+H}\frac{dz'}{1+E(z')}. \quad (63)$$

The first correction to the wavespeed obtained from Eq. (57) is as follows:

$$c^{(1)} = i\left[\frac{6}{5}\mathrm{Re} - \cot\beta - 9\Gamma\int_1^{1+H}\frac{dz'}{1+E(z')}\right]. \quad (64)$$

The quantity $c^{(1)}$, being a purely imaginary quantity, controls the growth of the disturbances and hence the stability of the system. The terms involving Re and cot β match exactly with those reported by Yih [2] as well as Shankar and Sahu [16] which further supports the validity of the present asymptotic solution.

The effect of the deformability of the solid layer on the free-surface instability in this limit can be understood with the term $9\Gamma\int_1^{1+H}\frac{dz'}{1+E(z')}$ and hence, we redefine the term using the "effective modulus" of the solid layer G_{eff}, which is given as

$$\frac{H}{G_{\mathrm{eff}}} = \int_1^{1+H}\frac{dz'}{E_0 + \overline{E}(z')}. \quad (65)$$

The effective modulus obtained for the continuous variation of shear modulus in a solid layer [Eq. (65)] is equivalent to the effective modulus of N solid layers having constant shear modulus, with thickness of each layer going to zero, and $N \to \infty$ such that the product of the thickness and N remains a constant:

$$\frac{H}{G_{\mathrm{eff}}} = \frac{H_1}{G_1} + \frac{H_2}{G_2} + \cdots + \frac{H_N}{G_N} = \sum_{i=0}^{N}\frac{H_i}{G_i}. \quad (66)$$

Here H_i represent the thickness of each solid layer and G_i represents the shear moduli. This suggests that a continuously varying shear modulus in a deformable layer can be treated as a generalisation of a multilayer system with with each layer having a different (but spatially uniform in a given layer) shear modulus. We further define $\Gamma_{\mathrm{eff}} = \overline{V_a}\mu/G_{\mathrm{eff}}R$ based on this effective shear modulus [Eq. (65)]. Thus, $c^{(1)}$ can be rewritten as

$$c^{(1)} = i\left[\frac{6}{5}\mathrm{Re} - \cot\beta - 9\Gamma_{\mathrm{eff}}H\right]. \quad (67)$$

The term $9\Gamma_{\mathrm{eff}}H$ occurs with a negative sign which suggests that solid layer deformability has a stabilizing effect on the free-surface instability. Physically, this would mean that in the long-wave-number limit, the deformations induced in the solid due to the tangential stress balance at the leading order (44), creates a perturbation flow near the liquid-solid interface that in turn opposes the fluid flow due to the inertia. This would lead to the stabilization of the free-surface instability. Also, it suggests that in the low-wave-number limit, it is the effective shear modulus that governs the stability of the system. In the limit of a rigid solid layer $G_{\mathrm{eff}} \to \infty$, and therefore Γ_{eff} approaches zero. Thus, from Eq. (67), we see that the contribution from the solid layer deformability vanishes as $\Gamma_{\mathrm{eff}} \to 0$. However, the free-surface instability is completely stabilized in the long-wave limit when

$$\left[\frac{6}{5}\mathrm{Re} - \cot\beta\right] < 9\Gamma_{\mathrm{eff}}H. \quad (68)$$

Similar results were obtained by Sahu and Shankar [20] in the context of deformable bilayer on the stability of gas-liquid interface. However, the predictions of the asymptotic analysis are valid only in the limit of $k \ll 1$. In the following section, the prediction of the analysis is extended to arbitrary values of wave number k by a numerical solution.

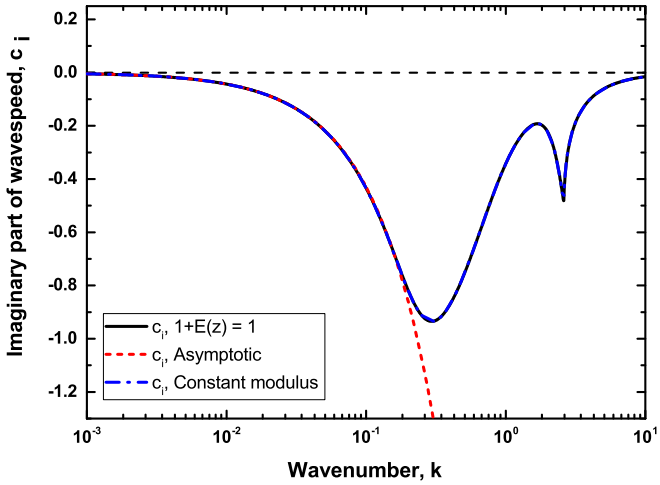

FIG. 2. Comparison of numerical results for continuous and constant modulus to low k asymptotic results: c_i vs k for $\beta = \pi/4$, $\mathrm{Re} = 1.0$, $H = 0.5$, $\Gamma_{\mathrm{eff}} = 1$. The horizontal line at $c_i = 0$ acts as a reference to differentiate between stable and unstable regions.

IV. RESULTS AND DISCUSSION

The Orr-Sommerfeld Eq. (15) for the velocity field in the fluid and the fourth-order differential equation for the displacement field (19) in the solid are solved numerically using the shooting technique [16]. The results were further verified using a spectral collocation method [28]. The eigenvalues obtained from both the methods agree to six significant figures. The imaginary part of eigenvalues obtained from the analysis is plotted against the wave number, in Fig. 2, to understand the origin and evolution of the instabilities in the $c_i - k$ plane. The numerical result demonstrates a perfect match with the low-wave-number asymptotic analysis until $k \sim 0.1$ and begins to differ from the asymptotic results from $k \sim 0.2$ onwards. Also the result matches exactly with those presented by Shankar and Sahu [16] for the given case, which further establishes the validity of the results. In Fig. 3, we

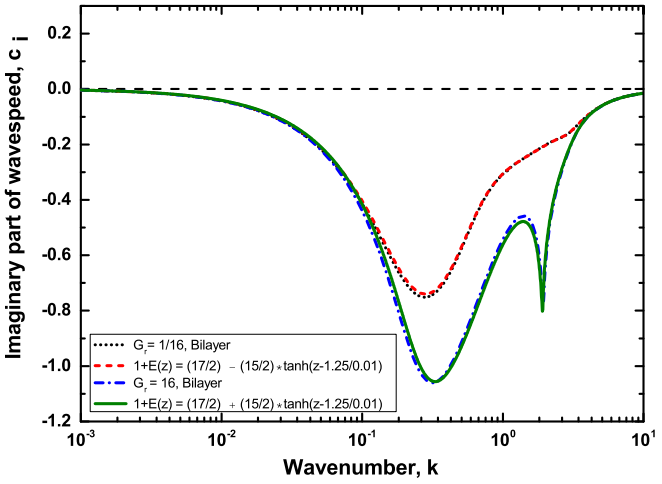

FIG. 3. c_i vs k variation for different solid configurations: $H = 0.5$, Re $= 1$, $\Gamma_{\text{eff}} = 1$, $\beta = \pi/4$, $b = 0.5$.

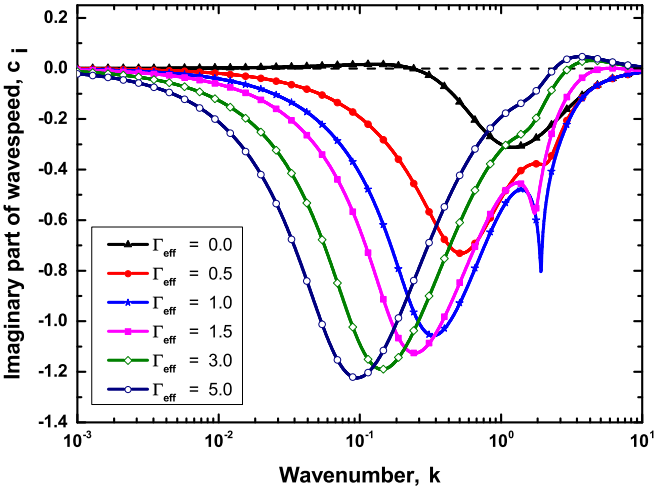

FIG. 4. c_i vs k variation for the GL mode for different values of Γ_{eff}: Data for $a_1 = 16$, $a_2 = 1$, $\beta = \pi/4$, Re $= 1.0$, $H = 0.5$, $b = 0.5$.

present the c_i versus k data for the modulus function of form

$$1 + E(z) = \frac{a_1 + a_2}{2} + \frac{a_1 - a_2}{2} \tanh\left(\frac{z - (1 + bH)}{\delta}\right). \tag{69}$$

Here a_1 and a_2 represent the value of the function at its two extremes and the parameter δ controls the steepness of the variation. The values of the parameters are chosen such that the tanh function imitates the step function as observed in the case of a bilayer of solid with two different moduli [20]. The results agree very well with the previous results for $G_r = 16$ and $1/16$ in the low-wave-number region, where G_r represents the ratio of moduli of the bottom to top-layer of the solid, in the bilayer configuration [20]. Also, there is a fair agreement between the curves in the finite-wave-number region which again establishes the validity of the use of the continuous modulus function as a generalization of the multiple solid layer system. We next present c_i versus k curves for different values of Γ_{eff} to understand the role of solid deformability on the stability of the system. In Fig. 4, for $\beta = \pi/4$, Re $= 1$, and $\delta = 0.01$, when the modulus at the liquid-solid interface is sufficiently low as compared to that at the bottom plate, we can easily see that for increasing values of Γ_{eff}, the system stabilises in low k region (as predicted from low-wave-number analysis). In the moderate k regime, the system stabilizes till $\Gamma_{\text{eff}} = 1$. In addition, the c_i versus k curves merge at high values of the wave number ($k \sim 10$) as the perturbations with high-k are confined near the free-surface at $z = 0$. Thus, the effect of solid deformability is expected to be minimal in the high-k limit. However, as the sold deformability is increased, the system starts to destabilize in this limit. Thus, increasing the Γ_{eff} value introduces the liquid-solid instability in the system, which was earlier absent in the case of flow over a rigid surface. The free-surface mode smoothly transitions to LS mode that leads to the destabilization of the flow in the high-k regime [16,17]. The results obtained are qualitatively similar to that of Sahu and Shankar [20].

To analyze the effect of the continuous variation of the shear modulus in the deformable solid, we define shear modulus using different functions such that the average modulus of all the functions remains the same. The spatially averaged shear modulus is defined as

$$G_{\text{avg}} = \frac{\int_1^{1+H} [1 + E(z)]dz}{\int_1^{1+H} dz}. \tag{70}$$

We next present results in the $c_i - k$ plane for a given function with different steepness, but same average modulus. Here we consider the modulus of the solid at the liquid-solid interface ($z = 1$) is sufficiently lower than the modulus at the rigid bottom plate ($z = 1 + H$). From Fig. 5, we observe that for the same values of modulus at the liquid-solid interface (Fig. 6), there is only a slight difference in the c_i versus k curve, in the finite k regime. Also, the c_i-k curves merge at sufficiently higher values of k, which establishes that the continuous variation of the modulus in a deformable solid has little role to play in determining the stability of the system for small wavelength fluctuations. Similarly, for the flipped modulus functions (i.e.,

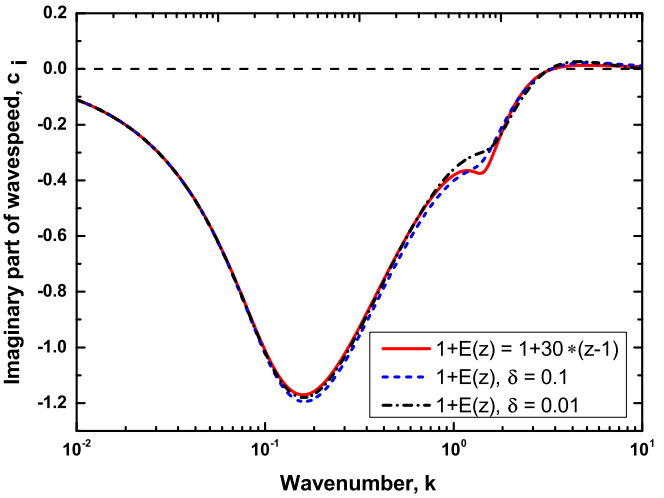

FIG. 5. c_i vs k variation for different values of δ: Data for $\beta = \pi/4$, Re $= 1.0$, $H = 0.5$, $\Gamma_{\text{eff}} = 2.5$, $b = 0.5$, $a_1 = 16$, $a_2 = 1$, and δ as mentioned in the figure.

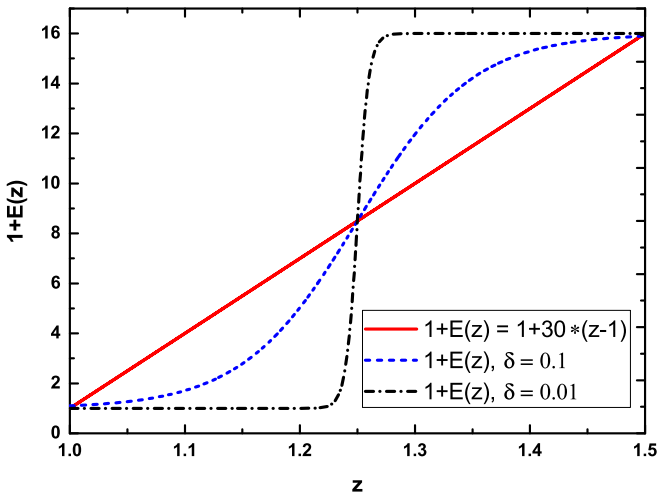

FIG. 6. Variation of the solid modulus with z: Data for $H = 0.5$, $b = 0.5$, $a_1 = 16$, $a_2 = 1$, and δ as mentioned in the figure.

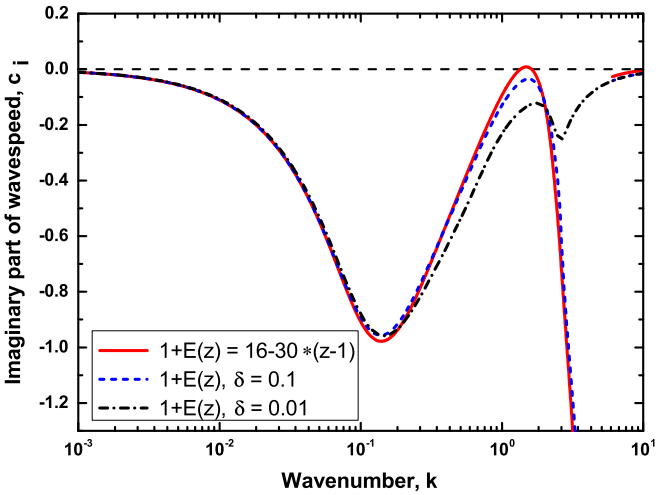

FIG. 8. c_i vs k variation for the different values of δ: Data for $\beta = \pi/4$, Re $= 1.0$, $H = 0.5$, $\Gamma_{\text{eff}} = 2.5$, $b = 0.5$, $a_1 = 1$, $a_2 = 16$, and δ as mentioned in the figure.

higher modulus at the liquid-solid interface; see Fig. 7) in Fig. 8, the c_i versus k curves merge in high-k regime, although they remain stable. This suggests that for the same value of effective shear modulus, a more stable case is the one having a higher modulus at the liquid-solid interface. A considerable difference between the curves can also be observed in the moderate-k regime ($k \sim 0.5$–5), which can further be used to manipulate the instabilities in this region. However, the complete picture can be obtained only with the help of neutral stability curves. We next present neutral curves (with $c_i = 0$) demarcating stable and unstable regions in the Γ_{eff}-k plane, demarcating the boundaries between the stable and unstable regions. This also helps us to identify the suitable range of the nondimensional parameter Γ_{eff} to induce or suppress the instabilities. Figure 9 represents the neutral stability curves for Re $= 1$, $\beta = \pi/4$ and multiple values of δ. For $\delta = 0.01$, as indicated by Fig. 6, the shear modulus function imitates the bilayer configuration for $G_r = 16$, whereas for other values of δ shear modulus varies smoothly within the solid layer. We also kept the average modulus of the function constant so as to have an appropriate comparison between the results.

We now proceed to analyze the effect of Γ_{eff} on the stability of the system. As Γ_{eff} is increased beyond 0.044 for the bottom left neutral stability curve, there is a transition from unstable to stable perturbations of the free surface mode. Similarly, if we consider the top right neutral stability curve, for a given wave number of 10, the free surface mode will undergo a transition from stable to unstable disturbances in the range of $\Gamma_{\text{eff}} \sim$ (1–3), depending upon the modulus function and δ value used. There is a large region in Γ_{eff} (for fixed values of other parameters), which translates into a large region in the shear modulus of the effective combination of the solid layer, where the free-surface mode is stabilized by the solid layer deformability. In Fig. 10 we considered the high shear modulus of a solid at the liquid-solid interface and low shear modulus at the bottom surface. As the value

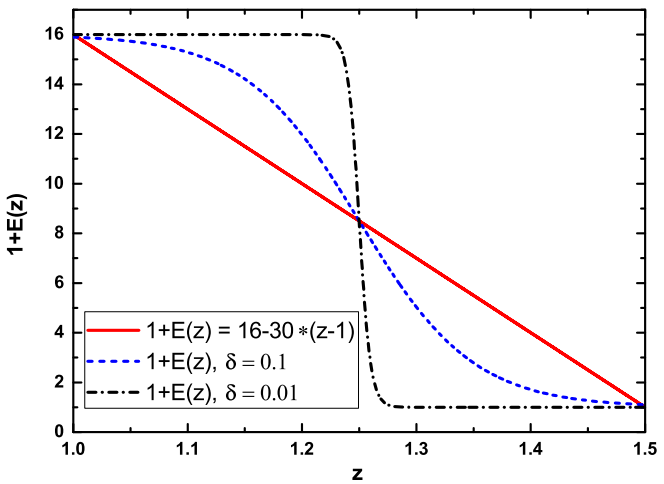

FIG. 7. Variation of the solid modulus with z: Data for $H = 0.5$, $b = 0.5$, $a_1 = 1$, $a_2 = 16$, and δ as mentioned in the figure.

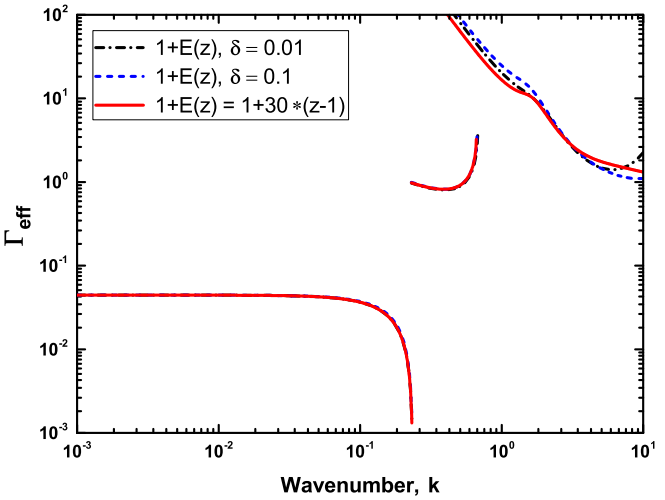

FIG. 9. Effect of δ on neutral stability curves in the Γ_{eff}-k plane: $\beta = \pi/4$, $b = 0.5$, Re $= 1.0$, $H = 0.5$, $a_1 = 16$, and $a_2 = 1$ and δ as mentioned in the figure.

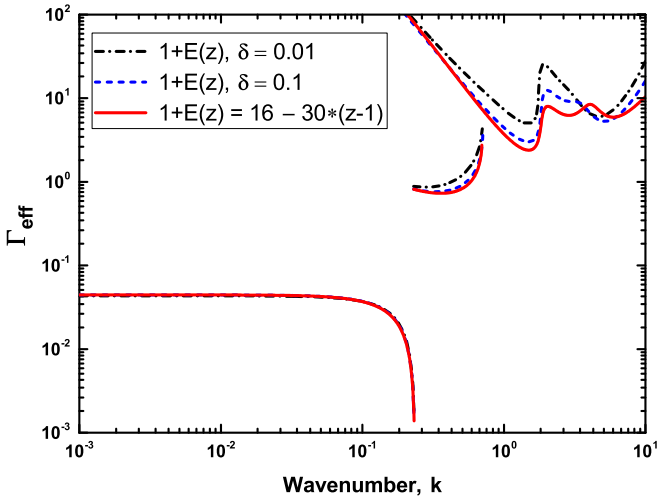

FIG. 10. Effect of δ on neutral stability curves in the Γ_{eff}-k plane: $\beta = \pi/4$, $b = 0.5$, Re $= 1.0$, $H = 0.5$, $a_1 = 1$, and $a_2 = 16$ and δ as mentioned in the figure.

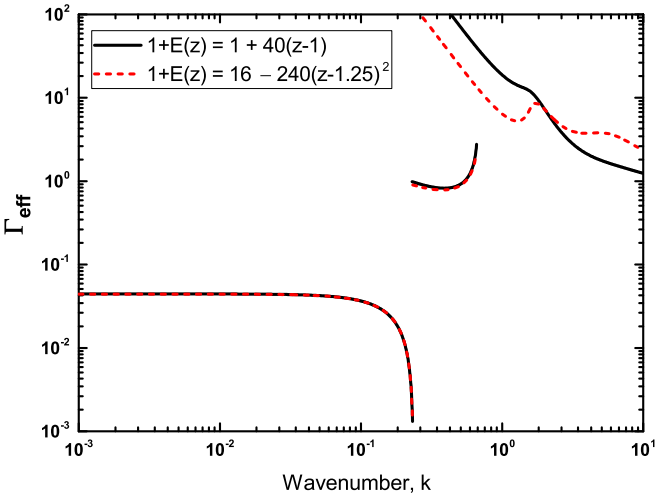

FIG. 12. Neutral stability curves in the Γ_{eff}- k plane showing the stability zones for the different solid modulus functions: Data for Re $= 1$, $H = 0.5$ and $b = 0.5$, $\beta = \pi/4$.

of δ is increased, the function smoothly transitions from a step function (mimicking the bilayer configuration) to a linear variation of shear modulus along the solid layer (Fig. 7). Here, we analyzed the role of solid deformability as well as the variation of the shear modulus function and observed two important features. First, the bottom left neutral curve for both the configurations overlaps exactly on each other and thus, in the low-wave-number region, only the effective modulus affects the stability of the system which reaffirms the asymptotic predictions as well. Second, in the high-wave-number region ($k \sim 1$), the Γ_{eff} values to destabilize the system is comparatively higher than those for low shear modulus at the liquid-solid interface (Fig. 9). Also, when we have the same shear modulus at the interface, the neutral stability curves move upwards, stabilizing the system for the cases having higher shear modulus near the liquid-solid interface.

We next examined the case of a nonmonotonous variation in the shear modulus of the deformable solid layer to ensure the dominance of the shear modulus near the liquid-solid interface on the stability of the system. In Fig. 11 we present two different configurations for the variation in the shear modulus in the solid layer along its depth. We consider a nonmonotonous variation in the shear modulus function of the form, $16 - 240[z - (1 + bH)]^2$ such that the functional value at the liquid-solid surface matches with that of the linearly increasing shear modulus function, $1 + 40(z - 1)$, and the average modulus for both the configurations is same. We compared the neutral stability curves in the $\Gamma_{\text{eff}} - k$ plane for both the variations in the shear modulus of the deformable solid layer as shown in Fig. 12. While the Γ_{eff} values for the low-wave-number limit overlap for both the modulus functions under consideration, in the high-wave-number regime we observe that the solid layer having the nonmonotonically varying modulus function is more stable as compared to the solid layer having the linearly increasing modulus function. This reaffirms our observation of the influence of the shear moduli near the liquid-solid interface on the stability of the system.

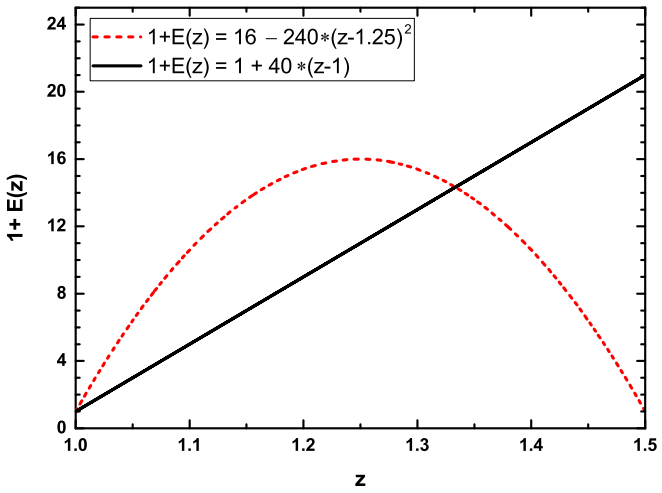

FIG. 11. Variation of the solid modulus with z: Data for $H = 0.5$ and $b = 0.5$.

V. CONCLUSION

In this work, we carried out a linear stability analysis of a gravity-driven flow of a Newtonian fluid past a linear elastic solid with depth-dependent modulus, lined on a rigid inclined plane. The results presented in this work significantly extend the prior work of Sahu and Shankar [20], carried out for elastic bilayers, to the case of a deformable solid with arbitrary depth-dependent modulus variations. As soft elastic solids are likely to have gradients in their shear modulus, by design or otherwise [26], our results generalize the earlier work to practically relevant situations. Following are the key findings of this analysis. First, we found from the low-wave-number asymptotic analysis that free-surface instability could be suppressed in the low-wave-number region, and it is governed only by the effective modulus of the solid layer Γ_{eff}, and is not sensitive to the details of variation in the

shear modulus with the depth of the solid. Thus for $k \ll 1$, suppression of instabilities is independent of the configuration of the deformable solid layer as long as the effective shear modulus (Γ_{eff}) remains the same. Also, the results agree very well with those of Sahu and Shankar [20] for low wave numbers, and a fair agreement between the results is observed at finite wave numbers, provided that the shear modulus function imitates the step function as appropriate for the case of a bilayer of solid with two different moduli. This suggests that a continuously varying modulus system can be used to analyze the effect of multiple solid layers on the stability of the system. Second, for finite wave numbers, for the same average modulus, the more stable case is the one having a higher modulus at the interface. However, when we consider the case of same shear modulus at the liquid-solid interface and same average modulus, the more stable case is the one having higher modulus just below the liquid-solid interface. In conclusion, this study presents a comprehensive picture of the effects of continuously varying shear modulus in the soft solid layer on the stability of free-surface flow, and the results could be relevant to applications involving elastic solids with spatially varying modulus.

[1] T. B. Benjamin, Wave formation in laminar flow down an inclined plane, J. Fluid Mech. **2**, 554 (1957).

[2] C. S. Yih, Stability of liquid flow down an inclined plane, Phys. Fluids **6**, 321 (1963).

[3] C. S. Yih, Instability due to viscosity stratification, J. Fluid Mech. **27**, 337 (1967).

[4] T. W. Kao, Role of viscosity stratification in the instability of two-layer flow down an incline, J. Fluid Mech. **33**, 561 (1968).

[5] D. S. Loewenherz and C. J. Lawrence, The effect of viscosity stratification on the stability of free-surface flow at low Reynolds Number, Phys. Fluids A **1**, 1686 (1989).

[6] K. P. Chen, The onset of elastically driven wavy motion in the flow of two viscoelastic liquid films down an inclined plane, J. Non-Newtonian Fluid Mech. **45**, 21 (1992).

[7] W. Y. Jiang, B. Helenbrook, and S. P. Lin, Inertialess instability of a two-layer liquid film flow, Phys. Fluids **16**, 652 (2004).

[8] V. Kumaran, G. H. Fredickson, and P. Pincus, Flow induced instability of the interface between a fluid and a gel at low Reynolds number, J. Phys. II France **4**, 893 (1994).

[9] V. Kumaran and R. Muralikrishnan, Spontaneous Growth of Fluctuations in the Viscous Flow of a Fluid past a Soft Interface, Phys. Rev. Lett. **84**, 3310 (2000).

[10] J. B. Grotberg and O. E. Jensen, Biofluid mechanics in flexible tubes, Annu. Rev. Fluid Mech. **36**, 121 (2004).

[11] J. B. Grotberg, Respiratory fluid mechanics, Phys. Fluids **23**, 021301 (2011).

[12] S. P. Lin, J. N. Chen, and D. R. Woods, Suppression of instability in a liquid film flow, Phys. Fluids **8**, 3247 (1996).

[13] W. Y. Jiang and S. P. Lin, Enhancement or suppression of instability in a two-layered liquid film flow, Phys. Fluids **17**, 054105 (2005).

[14] E. A. Demekhin, S. Kalliadasis, and M. G. Velarde, Suppressing falling film instabilities by Marangoni forces, Phys. Fluids **18**, 042111 (2006).

[15] V. Gkanis and S. Kumar, Instability of gravity-driven free-surface flow past a deformable elastic solid, Phys. Fluids **18**, 044103 (2006).

[16] V. Shankar and A. K. Sahu, Suppression of instability in liquid flow down an inclined plane by a deformable solid layer, Phys. Rev. E **73**, 016301 (2006).

[17] Gaurav and V. Shankar, Stability of gravity-driven free-surface flow past a deformable solid at zero and finite Reynolds number, Phys. Fluids **19**, 024105 (2007).

[18] A. Jain and V. Shankar, Instability suppression in viscoelastic film flows down an inclined plane lined with a deformable solid layer, Phys. Rev. E **76**, 046314 (2007).

[19] Gaurav and V. Shankar, Manipulation of interfacial instabilities by using a soft, deformable solid layer, Sadhana **40**, 1033 (2015).

[20] S. Sahu and V. Shankar, Passive manipulation of free-surface instability by deformable solid bilayers, Phys. Rev. E **94**, 013111 (2016).

[21] Gaurav and V. Shankar, Role of wall deformability on interfacial instabilities in gravity-driven two-layer flow with a free surface, Phys. Fluids **22**, 094103 (2010).

[22] B. Dinesh and S. Pushpavanam, Linear stability of layered two-phase flows through parallel soft-gel-coated walls, Phys. Rev. E **96**, 013119 (2017).

[23] G. Haacke, J. S. Brinen, and P. J. Larkin, Depth profiling of acrylic/melamine formaldehyde coatings, J. Coat. Technol. **67**, 29 (1995).

[24] R. P. Vito and S. A. Dixon, Blood vessel constitutive models–1995-2002, Annu. Rev. Biomed. Eng. **5**, 413 (2003).

[25] L. Landau and E. Lifshitz, *Theory of Elasticity* (Pergamon, New York, 1989).

[26] V. Gkanis and S. Kumar, Instability of creeping flow past a deformable wall: The role of depth-dependent modulus, Phys. Rev. E **73**, 026307 (2006).

[27] R. Neelamegam, D. Giribabu, and V. Shankar, Instability of viscous flow over a deformable two-layered gel: Experiment and theory, Phys. Rev. E **90**, 043004 (2014).

[28] J. P. Boyd, *Chebyshev and Fourier Spectral Methods*, 2nd ed. (Dover, New York, 2001).